Journal of Organometallic Chemistry 695 (2010) 2305–2310

Contents lists available at ScienceDirect

Journal of Organometallic Chemistry

journal homepage: www.elsevier.com/locate/jorganchem

Luminescent organotin complexes with the ligand benzil bis(benzoylhydrazone)

Elena López-Torres [a,*], Antonio L. Medina-Castillo [b], Jorge F. Fernández-Sánchez [b], M. Antonia Mendiola [a]

[a] Departamento de Química Inorgánica, Avenida Francisco Tomás y Valiente 7, Universidad Autónoma de Madrid, Cantoblanco, 28049-Madrid, Spain
[b] Departamento de Química Analítica, C/ Fuentenueva s/n, Universidad de Granada, 18071 Granada, Spain

ARTICLE INFO

Article history:
Received 5 May 2010
Received in revised form
29 June 2010
Accepted 1 July 2010
Available online 3 August 2010

Keywords:
Benzoylhydrazone ligands
Organotin
Crystal structure elucidation
Luminescence

ABSTRACT

Three organotin complexes have been synthesised by reaction of the ligand benzil bis(benzoylhydrazone) LH_2 with SnR_2Cl_2 or SnR_3Cl (R = Me, Bu, Ph). In all the compounds the ligand is doubly deprotonated and behaves as N_2O_2 tetradentate chelate, leading to distorted octahedral arrangements with the ligand in the equatorial plane and the organic groups in the axial positions. The complexes have been fully characterised by spectroscopic techniques including ^{13}C and ^{119}Sn NMR in solution and in the solid state, which confirm that the structure found in the solid state is retained in chloroform solution, and two of them by single crystal X-ray diffraction. The luminescent properties of the ligand and its complexes have also been tested as well as the effect of pH, the addition of acetone and the ionic strength over the luminescence intensity.

1. Introduction

Organotin compounds are amongst the most widely used organometallic compounds, and over the last decades they have been used in a wide range of industrial and agricultural applications such as pesticides, fungicides and anti-fouling agents [1,2]. The high amount of organotin derivatives used in agriculture explains the large accumulation of these compounds in the environment. While bans in developed nations have helped to decrease the overall incorporation of certain organotin species into the environment, other countries still produce and utilize huge amounts of these compounds [3,4].

Organotin toxicity is directly linked to the number and nature of the organic moiety. Highly substituted organotin compounds are known to be the most toxic (tri- and disubstituted organotins), with their toxicity decreasing when the length of the alkyl chain decreases, being independent of the counterions [5]. Organotin compounds can suffer environmental degradation (speciation) by physico-chemical factors (UV, pH) and can be metabolized by prokaryotic and eukaryotic organisms, and in spite of its relatively high dissociation energy (190–220 kJ/mol), the covalent Sn–C bond can be cleaved by a number of environmental sources, including chemical attacks (nucleophilic or electrophilic), UV radiation and dealkylation by bacteria [1,2].

Therefore, the preparation of compounds that could be used as sensors for organotin compounds is an interesting topic to pursue. Within these sensors, the design and synthesis of fluorescent molecular sensors that selectively and specifically respond to the presence of a given analyte (in particular metal ions) in a complex matrix, is a research area that has received much interest [6–15]. Applications can span from process control to environmental monitoring, food analysis and medical diagnosis. Chemosensors based on fluorescence offer many advantages over other types of sensors in terms of sensitivity, response time and cost, and they are of crucial importance for the development of methods for the detection and quantification of metal ions such as zinc [16,17], cadmium [18,19], lead [20,21], mercury [22,23] and tin [24].

Following our interest in the study of the reactivity of potentially tetradentate ligands, we have established that the coordinating behaviour depends both in the reaction conditions and the metal preferences [25–28]. Thus, in a previous paper we have reported the synthesis of the title bis(hydrazone) ligand as well as its complexes with several divalent metals, which depending on the metal, range from monomers to trinuclear helicates [29]. In this paper, the ligand benzil bis(benzoylhydrazone) is reacted with di and triorganotin(IV) chlorides to yield fluorescent organotin complexes that have been fully characterised. The luminescent properties have been evaluated to establish if the ligand could be used as a probe for detecting organotin species.

Among other, the main aim of this paper is the synthesis and optical characterization of the bis(hydrazone) ligand LH_2 and its organotin(IV) complexes, in order to obtain all the luminescent

* Corresponding author.
E-mail address: elena.lopez@uam.es (E. López-Torres).

0022-328X/$ – see front matter © 2010 Elsevier B.V. All rights reserved.
doi:10.1016/j.jorganchem.2010.07.002

information as a previous step for the immobilisation of LH_2 into a solid phase and to test its optical sensing response. For this reason, the synthesis of the complexes have been evaluated under different solvents, in order to establish the polarity of the solid support we can use, and the luminescent properties have been analysed changing several chemical conditions, such as pH, solvent or ionic strength.

2. Experimental section

2.1. General

Microanalyses were carried out using a LECO CHNS-932 Elemental Analyzer. IR spectra in the 4000–400 cm^{-1} range were recorded as KBr pellets on a Jasco FT/IR-410 spectrophotometer. Fast atom bombardment mass spectra were recorded on a VG Auto Spec instrument using Cs as the fast atom and *m*-nitrobenzylalcohol (*m*-NBA) as the matrix. ^1H and ^{13}C NMR spectra were recorded on a Bruker AMX-300 spectrometer using $CDCl_3$ as solvent and TMS as internal reference. ^{119}Sn NMR spectra were recorded in the same spectrometer and the chemical shifts are reported relative to $Sn(Me)_4$ as internal reference. ^{13}C CP/MAS NMR spectra were recorded at 298 K in a Bruker AV400WB spectrometer equipped with a 4 mm MAS NMR probe (magic-angle spinning) and obtained using cross-polarization pulse sequence. The external magnetic field was 9.4 T, the sample was spun at 10–14 kHz and spectrometer frequencies were set to 100.61 MHz. For the recorded spectra a contact time of 4 ms and recycle delays of 4 s were used. Chemical shifts are reported relative to TMS, using the CH group of adamantane as a secondary reference (29.5 ppm.). ^{119}Sn CP/MAS NMR spectra were obtained in the same spectrometer using spinning rates of 10–14 KHz, pulse delays of 30 s, contact times of 8 ms and TPPM high power proton decoupling. Chemical shifts are reported relative to $Sn(Me)_4$, using tin(IV) oxide as a secondary reference. Luminescence spectra and relative fluorescence intensity (R.F.I.) were carried out with a luminescence spectrometer Varian Cary-Eclipse fitted with a Xenon discharge lamp (peak power = 75 kW), Czerny-Turner monochromators, an R-928 photomultiplier tube, which is red sensitive even at 900 nm, with manual or automatic voltage control, using the Cary-Eclipse software for Windows 95/98/NT system.

2.1.1. Benzil bis(benzoylhydrazone), LH_2

The ligand was prepared following a previously reported procedure [29]. Selected spectroscopic data: ^1H NMR (300 MHz, $CDCl_3$, 25 °C): δ = 9.01 (s, 2H, NH), 7.83 (m, 4H, Ph), 7.40–7.22 (m, 16H, Ph) ppm. ^{13}C CP/MAS NMR (300 MHz, 25 °C): δ = 164.4 (CO), 147.5 (CN), 133.8, 132.3, 128.3, 123.8 (Ph) ppm. IR (KBr): 3232 (m), 3178 (m) ν(NH); 3063 (w) ν(CH); 1674 (s), 1643 (s) ν(CO), 1604 (w) ν(CN), 712, 687 (s) δ(Ph) cm^{-1}.

2.1.2. [$SnMe_2L$] **1**

To a solution containing 100 mg (0.22 mmol) of LH_2 in 5 mL of dichloromethane with four drops of Et_3N were added 52 mg (0.22 mmol) of $SnMe_2Cl_2$ dissolved in 5 mL of the same solvent and the deep orange solution was stirred overnight. The solution was evaporated to dryness and 20 mL of diethyl ether were added. The white precipitate corresponding to $Et_3N{\cdot}HCl$ was discarded and the orange solution was allowed to evaporate slowly until orange crystals suitable for X-ray analysis were obtained in good yield (122 mg, 92%). $C_{30}H_{26}N_4O_2Sn$ (592.91): calcd. C 60.72, H 4.42, N 9.45; found C 60.53, H 4.30, N 9.58. ^1H NMR (300 MHz, $CDCl_3$, 25 °C): δ = 8.08 (d, 4H, Ph), 7.54–7.22 (m, 16H, Ph), 0.98 (s, 6H, Me, $^2J_{Sn,H}$ = 94.0 Hz) ppm. ^{13}C NMR (300 MHz, $CDCl_3$, 25 °C): δ = 173.5 (CO), 148.7 (CN), 134.9, 132.2, 131.3, 130.8, 129.4, 128.6, 128.0, 127.4 (Ph), 4.9 (Me) ppm. ^{13}C CP/MAS NMR (300 MHz, 25 °C): δ = 172.5 (CO), 150.1 (CN), 134.5, 130.8, 129.4, 127.4 (Ph), 4.3 (Me) ppm. ^{119}Sn NMR (300 MHz, $CDCl_3$, 25 °C): δ = −261 ppm. ^{119}Sn CP/MAS NMR (300 MHz, 25 °C): δ = −275 ppm. IR (KBr): 3050 (w) $\nu(CH_{Ph})$, 2973 (w), 2938 (w) $\nu(CH_{Me})$, 1600 (w) ν(CN), 1585 (m) ν(CO), 712 (s), 688 (m) δ(Ph) cm^{-1}. MS (FAB^+): *m*/*z* (%) = 595.1 (100) $[M + H]^+$, 578.2 (15) $[M - Me]^+$. The same complex was obtained when $SnMe_3Cl$ was used.

2.1.3. [$SnBu_2L$] **2**

The complex was obtained following the same procedure described above but adding 70 mg (0.22 mmol) of $SnBu_2Cl_2$. Single crystals were also obtained from slow evaporation of the mother liquor. Yield: 132 mg, 87%. $C_{36}H_{38}N_4O_2Sn$ (677.01): calcd. C 63.81, H 5.66, N 8.27; found C 63.97, H 5.54, N 8.57. ^1H NMR (300 MHz, $CDCl_3$, 25 °C): δ = 8.10 (d, 4H, Ph), 7.47–7.26 (m, 16H, Ph), 1.74 (t, 4H, Bu), 1.55 (q, 4H, Bu), 1.32 (sx, 4H, Bu), 0.83 (t, 6H, Bu) ppm. ^{13}C NMR (300 MHz, $CDCl_3$, 25 °C): δ = 173.7 (C=O), 149.0 (C=N), 135.1, 132.5, 131.2, 130.7, 129.2, 128.7, 128.0, 127.5 (Ph), 27.6, 26.2, 25.4, 13.6 (Bu) ppm. ^{13}C CP/MAS NMR (300 MHz, 25 °C): δ = 174.7 (CO), 151.5 (CN), 136.7, 134.3, 131.7, 129.1 (Ph), 28.1, 27.5, 25.2, 14.5 (Bu) ppm. ^{119}Sn NMR (300 MHz, $CDCl_3$, 25 °C): δ = −284 ppm. ^{119}Sn CP/MAS NMR (300 MHz, 25 °C): δ = −273 ppm. IR (KBr): 3057 (w) $\nu(CH_{Ph})$, 2955 (m), 2924 (m), 2872 (m), 2857 (m) $\nu(CH_{Bu})$, 1598 (w) ν(CN), 1588 (m) ν(CO), 712 (s), 687 (s) δ(Ph) cm^{-1}. MS (FAB^+): *m*/*z* (%) = 679.2 (100) $[M + H]^+$, 620.9 (75) $[M - Bu]^+$, 568.1 (20) $[M - 2Bu + H]^+$. The same complex was synthesised starting from $SnBu_3Cl$.

2.1.4. [$SnPh_2L$] **3**

The complex was obtained following the same procedure described for complex **1** but adding 91 mg (0.22 mmol) of $SnPh_2Cl_2$. Yield: 151 mg, 74%. $C_{40}H_{30}N_4O_2Sn$ (716.95): calcd. C 66.95, H 4.22, N 7.81; found C 67.13, H 4.30, N 7.68. ^1H NMR (300 MHz, $CDCl_3$, 25 °C): δ = 8.18 (d, 8H, Ph), 7.78–7.71 (m, 8H, Ph), 7.50–7.23 (m, 24H, Ph) ppm. ^{13}C NMR (300 MHz, $CDCl_3$, 25 °C): δ = 172.1 (CO), 148.7 (CN), 136.2, 131.9, 130.9, 129.5, 128.9, 128.7, 128.1, 127.4 (Ph) ppm. ^{13}C CP/MAS (300 MHz, 25 °C): δ = 173.0 (CO), 151.3 (CN), 132.5, 128.4 (Ph) ppm. ^{119}Sn NMR (300 MHz, $CDCl_3$, 25 °C): δ = −235 ppm. ^{119}Sn CP/MAS NMR (300 MHz, 25 °C): δ = −240 ppm. IR (KBr): 3056 (w) $\nu(CH_{Ph})$, 1599 (w) ν(CN), 1586 (m) ν(CO), 732 (m), 712 (s), 693 (s), 688 (m) δ(Ph) cm^{-1}. MS (FAB^+): *m*/*z* (%) = 719.2 (100) $[M + H]^+$, 641.2 (40) $[M - Ph]^+$. The same complex was isolated when $SnPh_3Cl$ was used as the starting material.

The three complexes can also be synthesised in good yield in other solvents such as water, methanol or ethanol.

2.2. X-ray structure determination

Data for complexes **1** and **2** were acquired using a Bruker AXS Kappa Apex-II diffractometer equipped with an Apex-II CCD area detector using a graphite monochromator (Mo K_α radiation, λ = 0.71073 Å). The substantial redundancy in data allows empirical absorption corrections (SADABS) [30] to be applied using multiple measurements of symmetry-equivalent reflections. The raw intensity data frames were integrated with the SAINT program, which also applied corrections for Lorentz and polarization effects [31].

The software package SHELXTL version 6.10 was used for space group determination, structure solution and refinement. The structures were solved by direct methods (SHELXS-97) [32], completed with difference Fourier syntheses, and refined with full-matrix least-squares using SHELXL-97 minimizing $\omega(F_0^2 - F_c^2)$. Weighted *R* factors (R_w) and all goodness of fit *S* are based on F^2 and conventional *R* factors (*R*) are based on *F* [33]. All non-hydrogen atoms were refined with anisotropic displacement parameters and

the hydrogen atoms were positioned in idealised positions after each cycle of refinement. All scattering factors and anomalous dispersions factors are contained in the SHELXTL 6.10 program library.

3. Results and discussion

The reactions were carried out in dichloromethane at room temperature in the presence of Et_3N (Scheme 1), which is essential to induce the ligand deprotonation. As a result, a white crystalline material, $Et_3N{\cdot}HCl$, is formed but it can be eliminated due to its insolubility in diethyl ether. Elemental analysis of the complexes indicates a 1:1 ligand:tin ratio, as well as the absence of Cl^-. The same complexes were obtained starting from the triorganotin derivatives, as well as working in other solvents such as water or alcohols.

3.1. X-ray analysis

The crystal structure of complexes **1** and **2** have been determined and their crystallographic and refinement data are summarized in Table 1. In both complexes the ligand is doubly deprotonated and behaves as a tetradentate N_2O_2 chelate, coordination mode that leads to the formation of three five-membered chelate rings that confer high stability to the compounds. This coordination behaviour was previously reported for a nickel complex. By contrast, with lead and cadmium the ligand behaves also as a bridge through one of the oxygen atoms to form dinuclear complexes and with zinc and copper is pentadentate, but tridentate N_2O chelate to one metal and bidentate NO chelate to another to yield trinuclear helicates [29]. Table 2 shows the ligand bond lengths in the complexes as well as in the uncoordinated LH_2 [29]. It can be concluded that deprotonation of the ligand induces more electronic delocalisation.

The molecular structure of complex **1** consists of discrete molecules of $[SnMe_2L]$, in which the tin atom is in a strongly distorted octahedral arrangement with the deprotonated ligand in the equatorial plane and the methyl groups in the axial positions (Fig. 1, Table 3). There are not relevant differences between Sn–N bond distances, as well as happens with Sn–O and Sn–C bonds, and all of them are in the normal range found for this kind of complexes. The ligand skeleton can be considered planar with a maximum deviation from the least-squares plane of 0.059 Å for N(3). The phenyl rings of the hydrazone form dihedral angles with this plane of 24.96° for C(11)–C(16) and 8.08° for C(41)–C(46), while with the rings coming from benzil are 53.44° and 48.81° for C(21)–C(26) and C(31)–C(36) respectively.

Complex **2** crystallises in the chiral monoclinic group *Pc* as a racemic mixture. The asymmetric unit is made up by two crystallographically distinct units of $[SnBu_2L]$. There are no relevant differences in the bond lengths and angles (Tables 2 and 4), so in Fig. 2 is only depicted one of the molecules. The tin atom has the same coordination environment found in complex **1**. In each unit

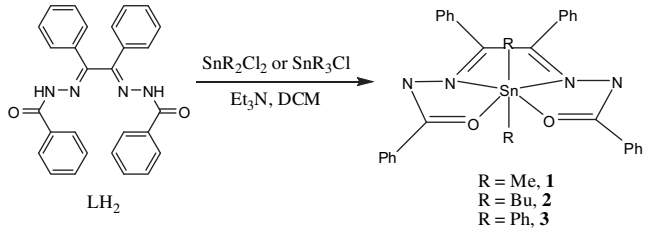

Scheme 1.

Table 1
Crystal and structure refinement data for complexes **1** and **2**.

	1	2
Formula	$C_{30}H_{26}N_4O_2Sn$	$C_{36}H_{38}N_4O_2Sn$
M	593.24	677.39
Crystal system	Orthorhombic	Monoclinic
Space group	*Pbca*	*Pc*
a/Å	10.1467(6)	10.4155(6)
b/Å	15.5452(9)	16.6850(9)
c/Å	33.127(2)	18.7548(10)
α/°	90	90
β/°	90	102.280(3)
γ/°	90	90
U/Å^3	5225.3(5)	3184.7(3)
Z	8	4
D_c/Mgm^{-3}	1.508	1.413
Absorption coefficient mm^{-1}	1.013	0.840
F(000)	2400	1392
Goodness of fit on F^2	0.988	1.083
Reflections collected	42262	45827
Independent reflections	6478 [*R*(int) = 0.0567]	13750 [*R*(int) = 0.0768]
Absolute structure parameter		0.49(3)
Final *R*1and *wR*2[$I > 2\sigma(I)$]	0.0312, 0.0766	0.0475, 0.1054
Residual electron density (min, max) (e Å^{-3})	−0.674, 0.688	−1.488, 1.127

the two butyl ligands have different conformation, while one of them is *anti* the other is *gauche*, probably due to the steric requirements of the phenyl rings. The ligands are less planar than in the methyl derivative, with one of the oxygens quite deviated from the least-squares plane formed by the rest of the skeleton. For the molecule containing Sn(1) the maximum deviation is 0.0913 Å for N(1) and O(1) is 0.44 Å above this plane and for the unit containing Sn(2) the maximum deviation is 0.062 Å for C(13) with O(3) 0.26 Å under the plane. The dihedral angles of the phenyl groups are similar to those found in complex **1**, 16.06° for C(11A)–C(16A), 49.35° for C(21A)–C(26A), 56.72° for C(31A)–C(36A), 8.70° for C(41A)–C(46A), 6.94 for C(51A)–C(56A), 46.19° for C(61A)–C(66A), 58.53° for C(71A)–C(76A) and 14.43° for C(81A)–C(86A).

3.2. IR spectroscopy

In all the complexes, coordination of the carbonyl group to the metal is confirmed by the shift of the *ν*(CO) band to lower frequencies compared with that of the free ligand. By contrast, the *ν*(CN) bands are not very shifted, but the crystal structure determination of complexes **1** and **2** confirm that the ligand is

Table 2
Selected bond distances (Å) of the ligand skeleton in LH_2 [29] and complexes **1** and **2**.

	LH_2	1	2
C(1)–O(1)	1.2225(15)	1.269(3)	1.295(9)
C(13)–O(3)			1.274(9)
C(1)–N(1)	1.3764(16)	1.340(3)	1.334(10)
C(13)–N(5)			1.335(9)
N(1)–N(2)	1.3753(15)	1.365(3)	1.363(8)
N(5)–N(6)			1.372(9)
C(2)–N(2)	1.2891(16)	1.308(3)	1.292(10)
C(14)–N(6)			1.307(10)
C(2)–C(3)	1.507(2)	1.482(3)	1.471(11)
C(14)–C(15)			1.508(11)
C(3)–N(3)	1.2891(16)	1.305(3)	1.307(10)
C(15)–N(7)			1.304(10)
N(3)–N(4)	1.3753(15)	1.375(3)	1.374(8)
N(7)–N(8)			1.396(8)
N(4)–C(4)/	1.3753(15)	1.331(3)	1.344(10)
N(8)–C(16)			1.331(9)
C(4)–O(2)	1.2225(15)	1.276(3)	1.277(9)
C(16)–O(4)			1.276(9)

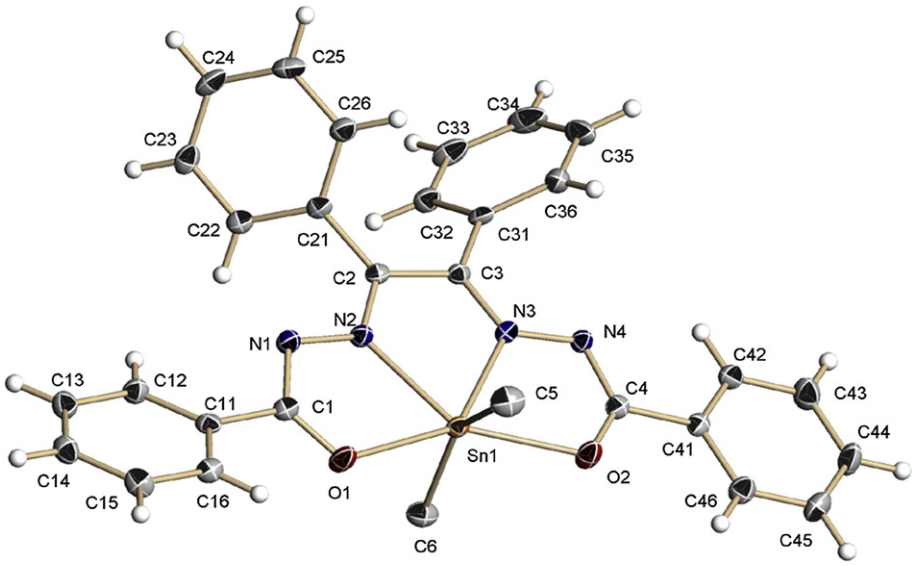

Fig. 1. Molecular structure of complex [$SnMe_2L$] **1**. Thermal ellipsoids at 50% probability. Hydrogen atoms of the methyl groups have been omitted for clarity.

tetradentate N_2O_2. Having a look at the bond distances found in the crystal structures it can be seen that while C=O bonds change considerably with respect to those of the free ligand, C=N bond distances are very similar, explaining the small shifts observed in the IR spectra.

3.3. NMR spectroscopy

The ^{1}H NMR spectra of the complexes confirm the ligand deprotonation, due to the loss of the signal corresponding to the NH groups, as well as the presence of the organic groups bonded to the tin. Satellites corresponding to the coupling with tin can only be observed in the spectrum of complex **1**. Substitution of $^2J_{Sn,H}$ value into the corresponding Lockhart–Manders equation [34] (empirical relationship between the coupling constants and the C–Sn–C angle) gives an angle of 154°, which is close to the value found in the crystal structure, 147°. This similarity indicates that the structure found in the solid state is retained in solution.

^{13}C NMR CP/MAS spectra of all the complexes show that the signals corresponding to the CO and CN are shifted with respect to the free ligand, indicating coordination of these groups to the tin. The CO bond signals are much more shifted than the CN ones, as happens with the IR spectra and what can also be explained with the X-ray diffraction data. The signals belonging to the organic groups are also observed. Comparison with the ^{13}C NMR spectra in solution indicates that the structure found in the solid state is retained in chloroform. The satellites corresponding to the $^1J_{Sn,C}$ cannot be observed in any spectrum, so the corresponding Lockhart–Manders equation could not be used to get the value of the C–Sn–C angle.

The ^{119}Sn chemical shift of tin complexes appear to depend not only on coordination number, but it is also very sensitive to the type of donor atoms bonded to the metal ion, so it is a useful tool to determine the chemical environment of the tin atom. In addition, solid-state NMR is an important technique to bridge the information gap between X-ray diffraction and solution NMR spectroscopic data. Holecek established for *n*-butyl derivatives that four-coordinate compounds have $\delta(^{119}Sn)$ values in solution ranging from δ +200 to −60 ppm, five-coordinate compounds from δ −90 to −190 ppm and six-coordinate compounds from δ −210 to −400 ppm [35]. The values found in solution (−261, −284 and −235 ppm, for complexes **1**, **2** and **3** respectively) and in the solid state (−275, −273 and −240 ppm) (see ESI) are within the range expected for six-coordinate complexes, which agree with the environments found in the crystal structures of **1** and **2**. The similarity in the ^{119}Sn chemical shifts found in solution and in the solid state indicates that the coordination environments of the three complexes do not change in chloroform solution.

Table 3
Selected bond distances (Å) and angles (°) for complex [$SnMe_2L$] **1**.

Sn(1)–N(2)	2.238(2)	Sn(1)–O(2)	2.2960(19)
Sn(1)–N(3)	2.246(2)	Sn(1)–C(5)	2.106(3)
Sn(1)–O(1)	2.2675(19)	Sn(1)–C(6)	2.117(3)
C(5)–Sn(1)–C(6)	147.63(11)	N(2)–Sn(1)–O(1)	69.40(7)
C(5)–Sn(1)–N(2)	106.07(10)	N(3)–Sn(1)–O(1)	140.17(7)
C(6)–Sn(1)–N(2)	100.32(10)	C(5)–Sn(1)–O(2)	85.61(10)
C(5)–−Sn(1)–N(3)	104.86(10)	C(6)–Sn(1)–O(2)	86.13(10)
C(6)–Sn(1)–N(3)	101.26(9)	N(2)–Sn(1)–O(2)	139.94(7)
N(2)–Sn(1)–N(3)	70.77(7)	N(3)–Sn(1)–O(2)	69.19(7)
C(5)–Sn(1)–O(1)	86.21(10)	O(1)–Sn(1)–O(2)	150.61(7)
C(6)–Sn(1)–O(1)	85.84(10)		

Table 4
Selected bond distances (Å) and angles (°) for complex [$SnBu_2L$] **2**.

Sn(1)–N(3).	2.237(6)	Sn(2)–N(7).	2.225(6)
Sn(1)–N(2)	2.240(7)	Sn(2)–N(6)	2.240(7)
Sn(1)–O(1).	2.283(5)	Sn(2)–O(3)	2.285(5)
Sn(1)–O(2)	2.290(5)	Sn(2)–O(4)	2.340(5)
Sn(1)–C(9)	2.128(8)	Sn(2)–C(21)	2.127(7)
Sn(1)-C(5)	2.144(7)	Sn(2)–C(17)	2.134(7)
C(9)–Sn(1)–C(5)	149.4(3)	C(21)-Sn(2)–C(17)	151.8(3)
C(9)–Sn(1)–N(3)	105.8(3)	C(21)–Sn(2)–N(7)	104.3(2)
C(5)–Sn(1)–N(3)	99.4(3)	C(17)–Sn(2)–N(7)	98.4(3)
C(9)–Sn(1)–N(2)	99.6(3)	C(21)–Sn(2)–N(6)	100.1(3)
C(5)–Sn(1)–N(2)	105.2(3)	C(17)–Sn(2)–N(6)	103.0(3)
N(3)–Sn(1)–N(2)	70.2(2)	N(7)–Sn(2)–N(6)	71.4(2)
C(9)–Sn(1)–O(1)	84.9(3)	C(21)–Sn(2)–O(3)	85.6(2)
C(5)–Sn(1)–O(1)	87.2(3)	C(17)–Sn(2)–O(3)	87.9(3)
N(3)–Sn(1)–O(1)	139.5(2)	N(7)–Sn(2)–O(3)	139.9(2)
N(2)–Sn(1)–O(1)	69.5(2)	N(6)–Sn(2)–O(3)	68.6(2)
C(9)–Sn(1)–O(2)	87.2(3)	C(21)–Sn(2)–O(4)	88.1(3)
C(5)–Sn(1)–O(2)	85.6(2)	C(17)–Sn(2)–O(4)	84.7(2)
N(3)–Sn(1)–O(2)	69.3(2)	N(7)–Sn(2)–O(4)	68.4(2)
N(2)–Sn(1)–O(2)	139.2(2)	N(6)–Sn(2)–O(4)	139.8(2)
O(1)–Sn(1)–O(2)	151.22(18)	O(3)–Sn(2)–O(4)	151.61(18)

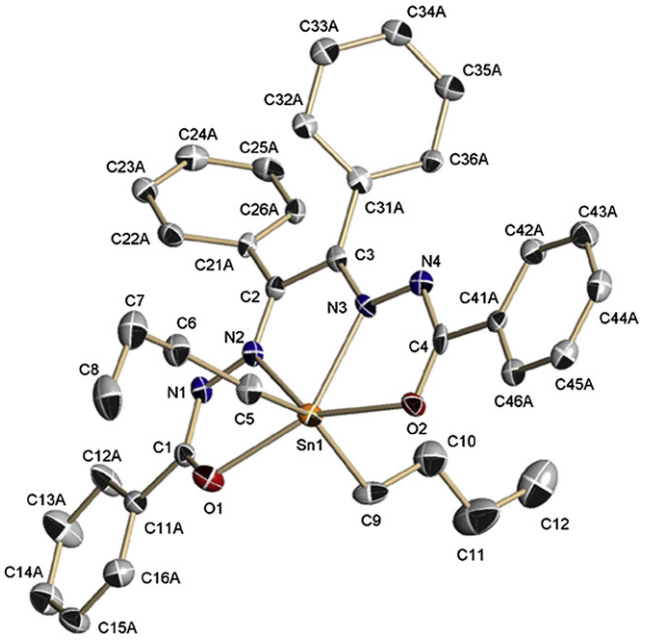

Fig. 2. Molecular structure of complex [$SnBu_2L$] **2**. Thermal ellipsoids at 50% probability. Hydrogen atoms have been omitted for clarity.

3.4. Mass spectrometry

All the complexes show the peak corresponding to the molecular mass $[SnR_2L + H]^+$, as well as the fragment corresponding to the loss of one of the organic groups $[SnRL]^+$. In the butyl derivative the peak corresponding to the loss of the two organic groups $[SnL + H]^+$ is also observed. In all the peaks the found and calculated isotopic patterns are identical.

Bearing these data in mind, we propose for complex **3** a structure analogous to that found for methyl and butyl derivatives, in which the metal is in a distorted $N_2O_2C_2$ octahedral arrangement (Scheme 1).

3.5. Luminescence spectroscopy

Table 5 shows the fluorescence properties of LH_2 and its complexes **1**, **2** and **3** in powder and in solution, and Fig. 3 shows the fluorescence excitation and emission spectra in solution of these compounds (Electronic supporting information, ESI, shows the excitation and emission spectra in powder). It can be observed that the complexes show an emission around 570 nm, while LH_2 emits at 415 nm. In addition, when the emission of LH_2 is recorded at the same conditions than the three complexes (see Table 5), it does not emit any luminescence (R.F.I. of LH_2 around 11 a.u.) while the complexes **1**, **2** and **3** provide R.F.I. signals of 635, 830 and 386 a.u., respectively. Thus, it can be concluded that the formation of the complexes provide an increase of the fluorescence emission with enhancement factors of 57, 75 and 35, respectively; therefore the ligand could be used as an optical probe for developing Sn-sensitive optical sensing.

Table 5
Luminescent properties of LH_2 and complexes **1**, **2** and **3**. $[LH_2] = [2] = [3] = 10^{-6}$ mol L^{-1}, $[1] = 10^{-5}$ mol L^{-1}, scan rate = 2 nm/s.

Luminescence properties	Powder				Solution			
	LH_2	**1**	**2**	**3**	LH_2	**1**	**2**	**3**
λ_{exc} (nm)	352	552	481,518	548	350	458	486	482
λ_{em} (nm)	414	590	551,573	600	412	566	566	572
$Slits_{exc/em}$	5/5	5/5	10/10	5/5	10/10	10/10	10/10	10/10
Detector voltage (V)	600	530	580	600	800	700	800	800
$pH_{optimum}$	–	–			7	5	5–9	5–9
$Acetone_{optimun}$ (%v.v.)	–	–			0	0	0	25

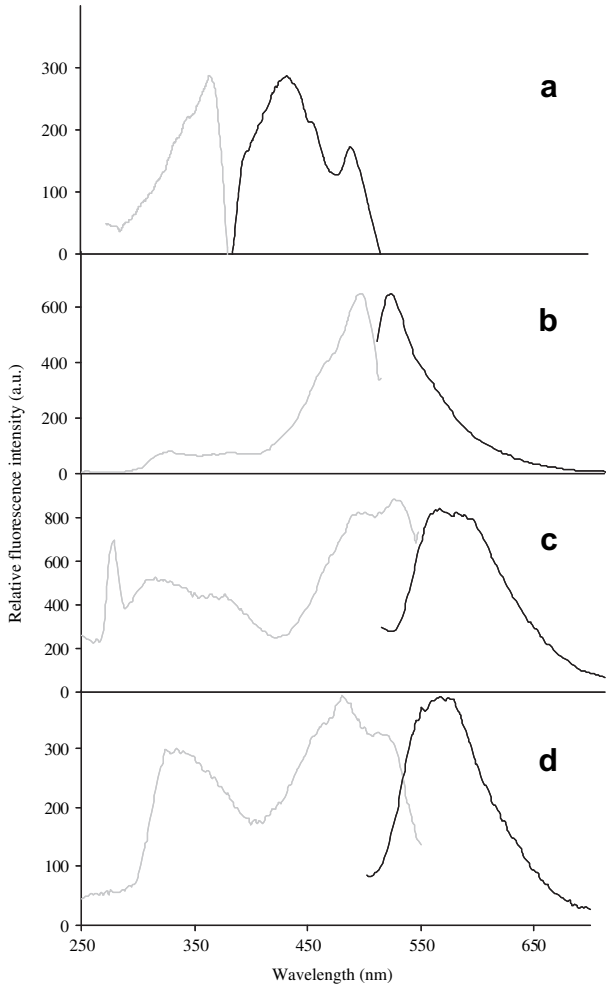

Fig. 3. Fluorescence excitation (grey line) and emission (black line) spectra of a) LH_2 b) complex **1**, c) complex **2** and d) complex **3** in solution. See Table 5 for experimental conditions.

The luminescent properties of the complexes are affected by the pH (see Fig. 4 and ESI). Complex **1** shows a maximum fluorescence emission at pH = 5; the maximum emission intensities of

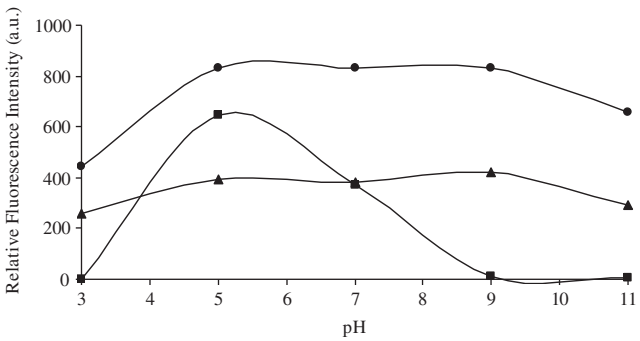

Fig. 4. Effect of the pH on the relative fluorescence intensity of complexes **1** (■), **2** (●) and **3** (▲). See Table 5 for experimental conditions.

complexes **2** and **3** are obtained between pH 5 and 9. Thus, strong acid or basic media provide a decrease of the fluorescence intensity for the three complexes. We have checked by ^{119}Sn NMR that addition of HCl leads to ligand protonation followed by complex decomposition, yielding SnR_2Cl_2 and LH_2. By contrast, addition of NaOH seems to have no effect on complex structures, but induces their precipitation.

With respect to the addition of acetone to the media (see ESI), complex **1** is not affected by the percentage of the organic solvent, complex **2** decreases its luminescence intensity when acetone is added to the media and complex **3** increases their fluorescent emission with the percentage of acetone.

The ionic strength has been also studied by adding NaCl at the optimum pH; it is possible to conclude that the ionic strength does not affect the fluorescence emission of any of the tested complexes (see ESI).

4. Conclusions

Reactions of the ligand benzil bis(benzoylhydrazone) LH_2 with SnR_2Cl_2 or SnR_3Cl (R = Me, Bu, Ph) in the presence of Et_3N yield three coordination compounds with general formula $[SnR_2L]$. In the complexes the tin atom is in a $N_2O_2C_2$ distorted octahedral environment formed by the doubly deprotonated ligand and the organic groups in the axial positions.

The complexes are fluorescent at different emission wavelength than LH_2, and complexation increases the fluorescent emission, what makes the ligand suitable as an optical probe for developing Sn-sensitive optical sensors.

Although further experiments have to be done in order to demonstrate its use as an optical probe to establish the applicability of the proposed ligand, it is possible to conclude that LH_2 should be used for detecting di and triorganotin(IV) species if it is immobilised in both a hydrophilic or hydrophobic material, because the complexes can be obtained in both media, but bearing in mind the optical properties, hydrophilic membranes could increase the luminescent sensitivity.

In addition, the pH into the solid support should be between 5 and 7, in order to increase the sensitivity, and lipophilic salts could be used without any problem to maintain the electroneutrality of the sensing layer, since the luminescence is not affected by the ionic strength of the media.

Concerning with the selectivity, it depends on the solid support used for making the sensing layer, thus it is one of the most important parameter to take into account in the design of the sensing layer and it should be very carefully study after the immobilisation of the chemosensing probe.

Acknowledgements

ELT and MAM thank to César J. Pastor for the crystal measurements and to MICINN, Instituto de Salud Carlos III, for funding (Project PS09/00963) ALMC and JFFS thank to the Junta de Andalucía for funding (Project P07-FQM-02738).

Appendix A. Supplementary material

CCDC numbers 755426 and 755427 contain the supplementary crystallographic data for complexes **1** and **2**, respectively. These data can be obtained free of charge from the Cambridge Crystallographic Data Centre via www.cdcc.cam.ac.uk/data_request/cif. Supplementary data associated with this article can be found, in the online version, at doi:10.1016/j.jorganchem.2010.07.002.

References

[1] M. Hoch, Appl. Geochem. 16 (2001) 719 (and references therein).
[2] B.A. Buck-Koehntop, F. Porcelli, J.L. Lewin, C.J. Cramer, G. Veglia, J. Organomet. Chem. 691 (2006) 1748 (and references therein).
[3] M.A. Champ, Sci. Total. Environ. 258 (2000) 1.
[4] S.M. Jenkins, S. Barone, Toxicol. Lett. 147 (2004) 63.
[5] S.M. Jenkins, K. Ehman, S. Barone Jr., Dev. Brain Res. 151 (2004) 1.
[6] Chemosensors of ions and molecular recognition. in: A.W. Czarnik, J.P. Desvergene (Eds.), NATO ASI Ser., Ser. C, Vol. 492. Kluwer Academic Publishers, Dordrecht, 1997.
[7] A.P. de Silva, H.Q.G. Gunaratne, T. Gunnlaugsson, A.J.M. Huxley, C.P. McCoy, J.T. Rademacher, T.E. Rice, Chem. Rev. 97 (1997) 1515.
[8] V. Amendola, L. Fabbrizzi, F. Foti, M. Licchelli, C. Mangano, P. Pallavicini, A. Poggi, D. Sacchi, A. Taglietti, Coord. Chem. Rev. 250 (2006) 273.
[9] E. Kimura, T. Koike, Chem. Soc. Rev. 27 (1998) 17.
[10] L. Prodi, F. Bolletta, M. Montalti, N. Zaccheroni, Coord. Chem. Rev. 205 (2000) 59.
[11] B. Valeur, I. Leray, Coord. Chem. Rev. 205 (2000) 3.
[12] R. Martínez-Máñez, F. Sancenón, Chem. Rev. 103 (2003) 441–449.
[13] J.S. Kim, D.T. Quang, Chem. Rev. 207 (2007) 3780.
[14] L. Basabe-Desmontes, D.N. Reinhoudt, M. Crego-Calama, Chem. Soc. Rev. 36 (2007) 993.
[15] C. Lodeiro, F. Pina, Coord. Chem. Rev. 253 (2009) 1353.
[16] M. Mameli, M.C. Aragoni, M. Arca, M. Atzori, A. Bencini, C. Bazzicalupi, A.J. Blake, C. Caltagirone, F.A. Devillanova, A. Garau, M.B. Hursthouse, F. Isaia, V. Lippolis, B. Valtancoli, Inorg. Chem. 48 (2009) 9236.
[17] Y. Weng, Z. Chen, F. Wang, L. Xue, H. Jiang, Anal. Chim. Acta 647 (2009) 215.
[18] H. Li, Y. Yao, C. Han, J. Zhan, Chem. Commun. (2009) 4812.
[19] L. Xue, C. Liu, H. Jiang, Org. Lett. 11 (2009) 1655.
[20] F. Zapata, A. Caballero, A. Espinosa, A. Tarraga, P. Molina, J. Org. Chem. 74 (2009) 4787.
[21] H.Y. Lee, D.R. Bae, J.C. Park, H. Song, W.S. Han, J.H. Jung, Angew. Chem. Int. Ed. 48 (2009) 1239.
[22] A. Jana, J.S. Kim, H.S. Jung, P.K. Bharadwaj, Chem. Commun. (2009) 4417.
[23] M.-L. Ho, K.-Y. Chen, G.-H. Lee, Y.-C. Chen, C.-C. Wang, J.-F. Lee, W.-C. Chung, P.-T. Chou, Inorg. Chem. 48 (2009) 10304.
[24] L. Qian, X.R. Yang, Adv. Funct. Mater. 17 (2007) 1353.
[25] E. López-Torres, M.A. Mendiola, C.J. Pastor, B. Souto Pérez, Inorg. Chem. 43 (2004) 5222 (and references therein).
[26] D.G. Calatayud, E. López-Torres, M.A. Mendiola, Inorg. Chem. 46 (2007) 10434 (and references therein).
[27] D.G. Calatayud, E. López-Torres, M.A. Mendiola, C.J. Pastor, J.R. Procopio, Eur. J. Inorg. Chem. (2005) 4401.
[28] D.G. Calatayud, E. López-Torres, M.A. Mendiola, Polyhedron 27 (2008) 2277.
[29] E. López-Torres, M.A. Mendiola, Dalton Trans. (2009) 7639.
[30] G.M. Sheldrick, SADABS Version 2.03, Program for Empirical Absorption Corrections. Universität Göttingen: Göttingen, Germany, 1997–2001.
[31] G.M. Sheldrick, SAINT+NT (Version 6.04) SAX Area-Detector Integration Program. Bruker AXS, Madison, WI, 1997–2001.
[32] G.M. Sheldrick, SHELXTL (Version 6.10) Structure Determination Package. Bruker AXS, Madison, WI, 2000.
[33] G.M. Sheldrick, Acta Crystallogr. Sect. A 46 (1990) 467.
[34] T.P. Lockhart, W.F. Manders, Inorg. Chem. 25 (1986) 892.
[35] J. Holecek, N. Nádvorník, K. Handlír, A. Lycka, J. Organomet. Chem. 315 (1986) 299.